

Article

Experimental Investigation on the Deformation Characteristics and Mechanical Behaviors of Tectonic Coal under Complex Unloading Confining Pressure

Deyi Gao ^{1,2,†}, Shuxun Sang ^{2,3,4,*,†} , Shiqi Liu ^{1,2,3,4,*}, Wenkai Wang ^{1,2} and Hang Mo ^{1,2}

¹ Key Laboratory of Coalbed Methane Resources and Reservoir Formation Process, China University of Mining and Technology, Xuzhou 221008, China

² School of Resources and Geosciences, China University of Mining and Technology, Xuzhou 221008, China

³ Carbon Neutrality Institute, China University of Mining and Technology, Xuzhou 221008, China

⁴ Jiangsu Key Laboratory of Coal-Based Greenhouse Gas Control and Utilization, China University of Mining and Technology, Xuzhou 221008, China

* Correspondence: shxsang@cumt.edu.cn (S.S.); liushiqi@cumt.edu.cn (S.L.)

† These authors contributed equally to this work.

Abstract: Conventional and cyclic unloading tests with different unloading rates were conducted to study the influences of unloading patterns and rates on the deformation characteristics and mechanical properties of tectonic coal. The results demonstrate that, under continuous unloading, a lower unloading rate promotes an increase in the circumferential strain but inhibits increases in axial strain. A lower unloading rate was found to be able to promote volume expansion under the cyclic unloading path, and the axial, circumferential, and volume strains increased stepwise with the unloading levels, but the increment of the strains decreased with the number of cycles in the same unloading level. It was easier for tectonic coal to reach the elastic limit by a low speed unloading rate when the unloading level was small, and volume dilatation was promoted when the unloading level was large. In both unloading patterns, the tangential modulus and the Poisson ratio were proportional to the unloading rate. Compared with continuous unloading, the cyclic unloading pattern was found to have a significant delaying and inhibiting effect on damage expansion, and thus higher mechanical strength and more structurally stable tectonic coal responses were observed.

Keywords: tectonic coal; unloading confining pressure; mechanical behavior; deformation characteristic



Citation: Gao, D.; Sang, S.; Liu, S.; Wang, W.; Mo, H. Experimental Investigation on the Deformation Characteristics and Mechanical Behaviors of Tectonic Coal under Complex Unloading Confining Pressure. *Energies* **2023**, *16*, 1889. <https://doi.org/10.3390/en16041889>

Academic Editor: Mohammad Sarmadivaleh

Received: 21 October 2022

Revised: 18 January 2023

Accepted: 23 January 2023

Published: 14 February 2023



Copyright: © 2023 by the authors. Licensee MDPI, Basel, Switzerland. This article is an open access article distributed under the terms and conditions of the Creative Commons Attribution (CC BY) license (<https://creativecommons.org/licenses/by/4.0/>).

1. Introduction

The original mechanical state of surrounding rock is broken in the mining process, resulting in the deformation and failure of the surrounding rock, which may lead to coal and gas outburst hazards [1–4]. Although it can cause dynamic disaster accidents in coal mines, the pressure relief of coal seams is of positive significance for the extraction of CBM [5]. Therefore, whether one wishes to ensure the safe exploitation of coal mines or to improve the extraction efficiency of coal bed methane (CBM), it is necessary to ascertain the mechanical behavior and deformation characteristics of rocks during the unloading confining pressure process [6].

Extensive work has been performed on analyzing the mechanical properties of coal and rocks during the unloading process under different unloading conditions (including unloading amplitude and rate), and many significant results have been obtained [7–9]. Sun et al. ascertained the meso-fracturing mechanism of marble under unloading confining pressure conditions by unloading confining pressure tests carried out in a laboratory and by numerical simulations [10]. Zhang et al. found that all of the ultimate intensity, peak strain, and residual stress increased gradually with the increase in the confining pressure unloading velocity [11]. The test results obtained by Ma et al. proved that the

fractal dimension of the coal fragmentation had a negative correlation with the initial unloading confining pressure, but a positive correlation with unloading rates [12]. Xue et al. investigated the effects of the unloading rate on the mechanical behavior and permeability evolution of the coal, and the results showed that the increase in the unloading rate reduced the compressive strength of the samples [13]. Some researchers believe that the new micro-cracks cannot extend or penetrate within a short time with the increase in the unloading rates [14]. Yin et al. showed that a higher unloading rate of the confining pressure corresponded to an earlier inflection point where the lateral expansion ratio changed from a decrease to an increase [15]. Jiang et al. studied the mechanical properties and seepage characteristics of intact coal under loading and unloading conditions, and, finally, an evolution model of permeability under loading and unloading conditions was developed, combined with a statistical damage model [16].

The permeability characteristics of coal samples during the unloading confining pressure process is another focus of attention. Pan et al. expressed the opinion that the unloading direction has a significant impact on the evolution of the permeability of coal [17]. Taking briquette samples as the object of study, Zhao et al. investigated the evolution of the mechanical parameters of coal containing gas using triaxial unloading confining pressure tests, and the results showed that the evolution of mechanical parameters of coal containing gas can be divided into two stages [18]. Yang et al. conducted a seepage test under a tiered cyclic unloading–loading confining pressure, and suggested that the unloading level and cyclic number have a significant influence on the deformation and permeability characteristics of raw coal [19].

Zhou et al. carried out creep experiments of coal under unloading confining pressure, and the results showed that the permeability decreased in the primary creep stage, remained stable in the steady creep stage, and increased rapidly in the accelerated creep stage [20]. In addition, Chen et al. reported the criterion for rock bursts based on the energy principles obtained from unloading confining pressure experiments [21]. Although many significant results have been obtained, most of the studies did not consider the effect of multiple repeated unloadings and loadings at the same stress level on the damage of coal.

Tectonic coal is widely distributed in China, and the amount of tectonic TCBM (tectonic coalbed methane) resources accounts for a large proportion of the total amount of CBM (coalbed methane) resources [22,23]. However, low strength and permeability are the main characteristics of tectonic coal. The current CBM exploitation theory of dewatering–depressurization–desorption is unfit for tectonically deformed coal seams. Sang Shuxun et al. presented the horizontal well cavern completion and stress relief theory, which provides a broad idea for the mining of tectonic coal [22]. Therefore, determining the deformation and failure characteristics of tectonic coal under confining pressure relief and maintaining the stability of boreholes is the key to achieving efficient extraction of TCBM. Most of the previous studies have focused on monotonous unloading experiments of intact coal, and few examples of research have focused on the mechanical properties under unloading confining pressure paths, especially on the internal mechanisms of tectonic coal deformation and failure under cyclic confining pressure. Under special circumstances, however, rocks will inevitably experience cyclic unloading–loading confining pressures (such as during drilling operations and artificial crushing of coal reservoirs), and cyclic unloading and continuous unloading are two completely different stress paths that produce dramatic differences in the deformation and failure modes of coal and rock masses [11,19].

In this study, mechanical behavior tests of tectonic coal samples under cyclic and continuous unloading paths were conducted using a rock mechanics test system, and we investigated the strength, mechanical parameters, and deformation behavior. The experimental results offer a meaningful understanding of the mechanical behavior and deformation evolution of tectonic coal seams during gas extraction projects.

2. Experimental Design and Schemes

2.1. Tectonic Coal Specimens

Reconstituted coal specimens are widely used in methane permeability and mechanical behavior tests for tectonic coal [24]. The original pulverized coal used in this study was obtained from the 11-2 coal seam of Zhangji mine, Huainan coalfield. After picking out gangue and coal briquettes, pulverized coal was poured into a vibrating screen, and the sifter mesh diameters were 4 mm, 1.7 mm, 0.88 mm, 0.425 mm, 0.325 mm, 0.25 mm, 0.18 mm, 0.15 mm, and 0.075 mm. After several repeats, the average value was used to replace the mass percentage of each particle size stage. The particle size distribution is shown in Table 1. Then, we placed the pulverized coal into the steel mold to make a cylinder sample with a diameter of 50 mm and a height of 100 mm, as shown in Figure 1. The pulverized coal was placed into a steel mold and formed pressure was provided by an electric-hydraulic serving compression machine. Then, we placed the samples in an oven until there was no change in weight.

Table 1. Mass percentage of pulverized coal with different particle size.

Mass Percentage of Pulverized Coal with Different Particle Size					
Diameter/mm	2–4	1–2	0.5–1	0.355–0.5	0.25–0.355
Percentage/%	35.5	27.72	18.74	3.58	7.06
Diameter/mm	0.18–0.25	0.15–0.18	0.075–0.15	<0.075	/
Percentage/%	2.49	1.91	1.81	1.19	/

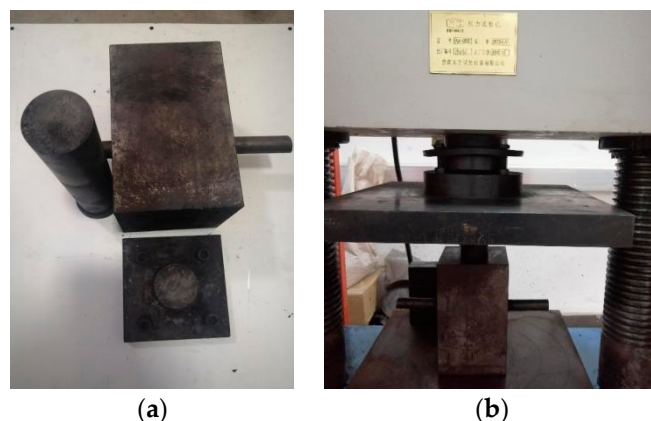


Figure 1. Steel mold and electric-hydraulic serving compression machine. (a) Steel mold; (b) electric-hydraulic serving compression machine.

2.2. Test Equipment

The MTS815 test system for rock mechanics from the State Key Laboratory for Geomechanics and Deep Underground Engineering (China University of Mining and Technology, Xuzhou, China) was used in this test, which consisted of the loading, testing, and control systems. The rigidity of the test machine was 10.5×10^9 N/m, and the upper limit of the confining pressure was 45 MPa, as show in Figure 2. The axial strain obtained by recording the displacement of the squeeze head and the circumferential strain was measured using an extensometer. The sampling interval in this experiment was 1 s.

The CT scans were performed using the high-resolution 3D X-ray microscopy imaging system: X-ray tube voltage was 30–60 KV, the X-ray power was 2–10 w, and the resolution ratio was 50 μ m. The 3D X-ray microscopy imaging system is affiliated to the Advanced Analysis and Computation Center (China University of Mining and Technology, Xuzhou).



Figure 2. MTS815 test system.

2.3. Test Procedure and Schemes

The experimental scheme included two paths and stress control was adopted, as show in Figure 3 and Table 2. First, the axial and confining pressures were increased simultaneously at 0.2 MPa/s until they reached 12 MPa. Then, unloading the confining pressure was commenced.

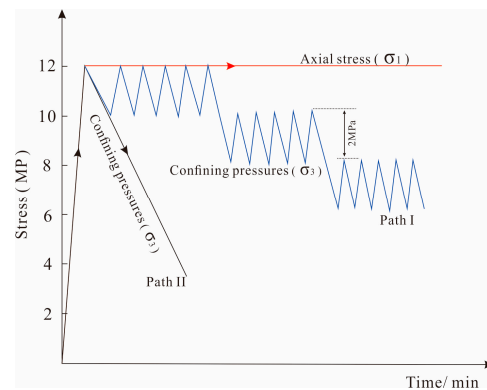


Figure 3. Unloading path.

Table 2. Test procedure and schemes.

Specimen	Unloading Path		
	Pattern	Rate	Gradient
B-1	Continuous unloading	0.25 MPa/min	/
B-2		1 MPa/min	/
C-1	Cyclic unloading	0.25 MPa/min	2 MPa
C-2		1 MPa/min	2 MPa

Path I:

Keeping the axial stress constant (12 MPa) and reducing the confining pressure; the lower limit confining pressure decreased by 2 MPa per gradient, and the unloading rates were 0.25 MPa/min and 1 MPa/min, respectively.

Path II:

Keeping the axial stress constant (12 MPa), continuously unloading the confining pressure at the same unloading rate as that of path I.

When the circumferential strain exceeded the stretching measurement range, we stopped the unloading immediately.

3. Results

3.1. Stress–Strain Curve

Figure 4 presents the stress–strain curves of tectonic coal in the cyclic unloading confining pressure test. With different unloading rates and patterns, the specimens exhibited similar deformation and failure characteristics in the overall triaxial test. However, in more detail, the difference between them was obvious. The deformation process under cyclic unloading confining pressure conditions can be divided into three phases: the compression phase, the slow expansion phase, and the accelerated expansion phase; however, the deformation process under the continues unloading confining pressure conditions can only be divided into the slow expansion phase and the accelerated expansion phase.

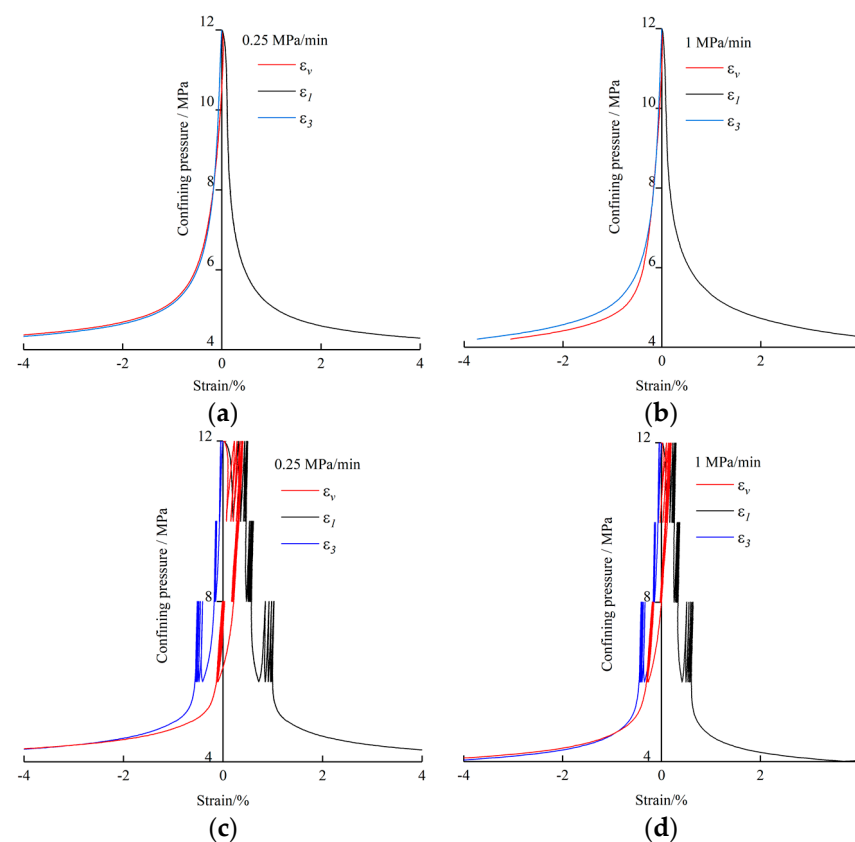


Figure 4. Stress–strain curves under different loading paths: (a) B-1; (b) B-2; (c) C-1; (d) C-2. ϵ_1 , ϵ_3 , ϵ_v are axial strain, circumferential strain, and volumetric strain, respectively, and from here onwards.

Path I:

In the compaction phase (the first unloading level), the interspace between the coal particles and micro-fissures inside the particles was compressed by the axial direction. In this process, the radial strain of the specimens was small, while the axial strain was relatively large, so the volume decreased with the continuous cyclic unloading. During the slow expansion stage (the second and third unloading levels), the deformation changed from compression to expansion. At the beginning of this stage, the volume of the sample did not expand much as compared with the initial state. For the C-1 specimen, the confining pressure lower than 7.8 MPa was the boundary of compression and shear, while for the C-2 sample, this value was 6.2 MPa. When the confining pressure was reduced to 5 MPa, the deformation entered the accelerated expansion stage.

The evolution of the circumferential and volumetric strains of the samples under triaxial cyclic unloading confining pressure at different levels corresponds to Figure 4 and is plotted in Figure 5. For each level, the strain in the first cycle was much larger than that of the subsequent cycles. Under the first unloading level, the sample volume was rapidly compressed, but the radial strain did not increase significantly. At the third stress level, however, the increment of radial strain was much higher than that of volume strain. In addition, under the same stress level, the width of the circumferential strain hysteresis curve increased with the increase in the number of cycles.

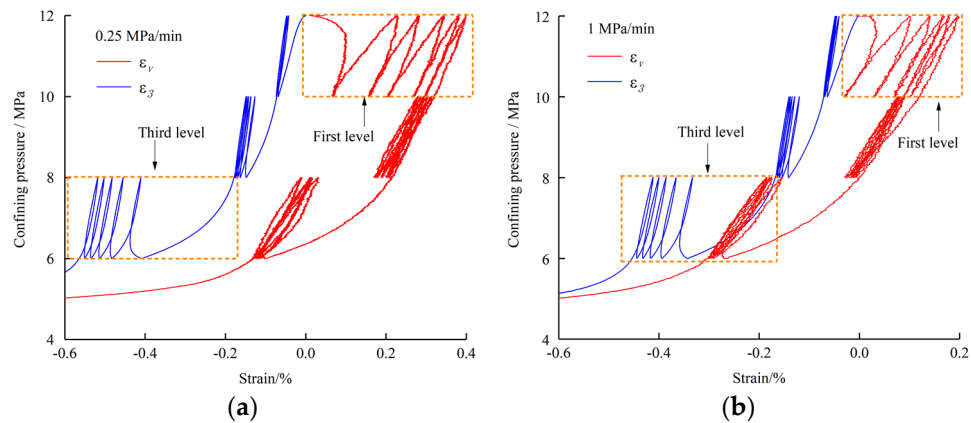


Figure 5. Circumferential and volumetric strain of cyclic unloading condition: (a) C-1; (b) C-2.

Path II:

Under the continuous unloading path, the axial strain increased slowly, and the circumferential strain increased negatively until the confining pressure was gradually applied to about 6 MPa. Then, with the further reduction in confining pressure, the axial and circumferential strain increased rapidly.

3.2. Irreversible Strains

Owing to the natural defects of rocks, natural rock material is not a perfectly elastic material. Even if the external forces are removed, deformation during the loading process cannot be completely recovered, and the gap between the final state and initial state is called an irreversible strain. In this experiment, the irreversible strain in a single cycle was equal to the strain at the end of the cycle minus the strain at the beginning, as show in Figure 6; Equation (1) shows the calculation method for the irreversible deformation of the tectonic coal samples.

$$\begin{cases} \epsilon_{1,I}^i = \epsilon_{1,L}^i - \epsilon_{1,F}^i \\ \epsilon_{3,I}^i = \epsilon_{3,L}^i - \epsilon_{3,F}^i \\ \epsilon_{V,I}^i = \epsilon_{V,L}^i - \epsilon_{V,F}^i \end{cases} \quad (1)$$

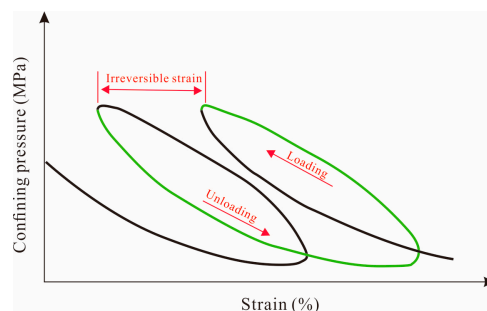


Figure 6. Irreversible strain in a single cycle.

$\varepsilon_{1,I}^i$, $\varepsilon_{3,I}^i$, and $\varepsilon_{V,I}^i$ refer to the axial, circumferential, and volumetric irreversible strain in a single cycle, respectively, and the I means the i -th cycle; $\varepsilon_{1,L}^i$, $\varepsilon_{1,F}^i$ represents the axial strain recorded at the last and first sampling point of the i -th cycle; the notation for circumferential and volumetric strains can be named in the similar manner.

Table 3 shows the irreversible strain in a single cycle. The axial irreversible strain was positive, and the circumferential irreversible strain was negative; the increment of the irreversible strain gradually decreased with the increase in the cycle times. Although the development of irreversible volume strain is complicated, in the first stage, the increments of the irreversible strain were positive, indicating that the sample was compressed during this stage, but the increments of contraction decreased with the increase in cycles times. During the second stage, the volume of the sample expanded during the first unloading cycle but converted to compression from the second cycle. When the unloading entered the third stage, although the growth was very slow, the tectonic coal had the tendency to expand with the increase in the number of cycles.

Table 3. Irreversible strain in a single cyclic.

Unloading Stage	Cycle Number	1 MPa/min			0.25 MPa/min		
		$\varepsilon_{1,I}^i$	$\varepsilon_{3,I}^i$	$\varepsilon_{V,I}^i$	$\varepsilon_{1,I}^i$	$\varepsilon_{3,I}^i$	$\varepsilon_{V,I}^i$
First stage	1	0.182	−0.037	0.109	0.293	−0.043	0.208
	2	0.048	−0.005	0.038	0.063	−0.003	0.056
	3	0.031	−0.001	0.028	0.062	−0.001	0.060
	4	0.012	−0.0007	0.010	0.038	−0.0001	0.037
	5	0.019	−0.0002	0.018	0.019	−0.00004	0.020
Second stage	1	0.059	−0.049	−0.039	0.067	−0.054	−0.042
	2	0.016	−0.009	0.002	0.027	−0.010	0.007
	3	0.014	−0.005	0.004	0.018	−0.005	0.008
	4	0.018	−0.004	0.011	0.017	−0.004	0.009
	5	0.003	−0.002	0.001	0.017	−0.003	0.011
Third stage	1	0.178	−0.17	−0.152	0.281	−0.232	−0.183
	2	0.043	−0.033	−0.022	0.073	−0.044	−0.015
	3	0.035	−0.020	−0.005	0.050	−0.027	−0.004
	4	0.023	−0.014	−0.006	0.044	−0.020	0.0044
	5	0.024	−0.011	0.001	0.005	−0.016	−0.027

4. Discussion

4.1. Influence of Unloading Rate on Deformation and Mechanical Characteristic

4.1.1. Influence on the Strain

Figure 7a,b show the stress–strain curves of the B-1 and B-2 specimens. The stress–strain curves of the axial, radial, and volume strains of the two samples almost coincided before the confining pressure was unloaded to 8 MPa. Compared with the B-1 specimen (0.25 MPa/min), when the confining pressure was unloaded to 6 MPa, the axial strain of the B-2 specimen (1 MPa/min) was slightly larger, while the radial strain was slightly smaller. Therefore, the volume expansion increment of B-2 was correspondingly smaller than that of B-1. However, with the further reduction in confining pressure, the gap became wider. When the confining pressure was 5 MPa, the gap of axial strain, radial strain, and volume strain between B-1 and B-2 were 0.295%, −0.095%, and −0.455% (Figure 7a,b), respectively. This indicated that, under the continued unloading conditions, the increase in the unloading rate was conducive to the increase in the axial strain, but it inhibited the increase in radial strain. Moreover, the slower the unloading speed, the larger the volume expansion.

Therefore, under the continuous unloading path, for axial and radial strains, the unloading rate changes have little influence on the structural coal strain. Only when the unloading rate of confining pressure is greater than 50%, the two strains show a positive correlation with the unloading rate. The volume strain is more sensitive to the variation of

unloading efficiency. When the unloading rate is greater than 33.33%, the growth rate of the volume strain of C-1 is significantly higher than that of C-2.

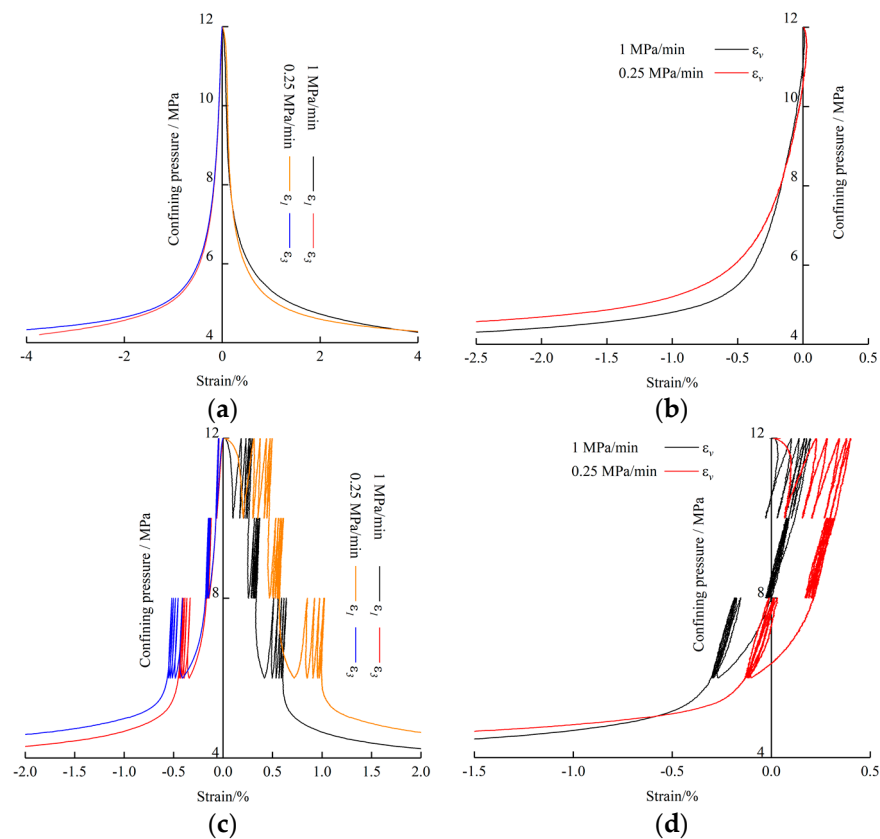


Figure 7. Stress–strain curves under different unloading rates: (a) axial and radial strains of B-1 and B-2; (b) volume strain of B-1 and B-2; (c) axial and radial strains of C-1 and C-2; (d) volume strain of C-1 and C-2.

Figure 7c,d show the stress–strain curves of C-1 and C-2. At the end of the first unloading stage, the axial strains of C-2 (1 MPa/min) and C-1 (0.25 MPa/min) were 0.245% and 0.443%, respectively. This indicated that the initial void in the sample was more fully compressed due to the lower unloading rate during the compression stage. Then, the gap between the two steadily increased and reached 0.380% at the end of the third unloading stage. During the first two unloading stages, the circumferential strains of C-1 were slightly larger than those of C-2. Entering the third unloading stage, the gap between the two curves gradually increased, and the slower the unloading rate, the faster the strain growth. According to the shape of the curve, the hysteresis loop in the stress–strain curve of C-1 was slightly wider than that of C-2; in other words, the volume expansion rate of the samples under a low unloading velocity was higher than that when under a high unloading velocity. Moreover, with the increase in the unloading degree, the promotion of a low unloading rate on the volume expansion of the tectonic coal was more obvious. For example, the volumetric strains of C-2 and C-1 were -0.0013% , -0.303% and 0.216% , -0.131% respectively, at the end of the second and third unloading stages. Compared with the initial volume, the dilatancy of C-2 occurred when the confining pressure dropped to 8.33 MP, while the corresponding confining pressure for C-1 was 6.35 MP. This does not mean that a lower unloading rate will inhibit the expansion of the specimen, but the compression of C-1 in the compaction stage was much greater than that of C-2.

Based on the above analysis, under cyclic unloading path, the axial strain and volume strain of tectonic coal are sensitive to unloading rate, while the unloading rate has a weak influence on radial strain. In each cycle, the axial strain increases in direct proportion to

the unloading rate. The increase in radial strain is almost not affected by the change of unloading rate before the acceleration increases stage. Only when the confining pressure is unloaded to 6 MPa, the growth of radial strain of C-1 is slightly higher than that of C-2. For volume strain, the lower the unloading rate is, the greater the compressive capacity of structural coal is in the initial unloading stage. As the confining pressure drops from 10 MP to 6 MP, the volume strain curves of the two samples are approximately parallel, indicating that there is no obvious correlation between the evolution of volume strain and unloading rate at this stage. Similar to the radial strain, the volume strain increases faster at a lower unloading rate when the confining pressure is less than 6 MPa.

4.1.2. Influence on the Tangential Modulus

The elastic modulus can reflect the deformation resistance of rocks; to a certain extent, it can also be used to describe the progressive damage during deformation and development in the rock mass. Owing to positive effects such as strain hardening and negative effects such as hysteresis, viscosity, and unloading damage, there are significant differences in the rock's tangential elastic modulus under different unloading and loading histories and paths; therefore, the tangent modulus is usually used in place of elastic modulus [25]. The calculation method of the tangential modulus (E_T) used in this study is shown in Figure 8.

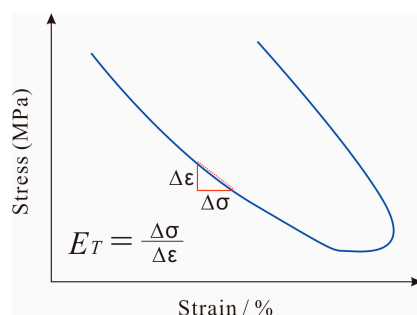


Figure 8. Schematic diagram of tangential modulus.

Under the continuous unloading path, the tangential modulus first increased and then decreased (Figure 9a), and the peak values of B-1 and B-2 (3.54 GPa and 3.69 GPa, respectively) appeared when the confining pressures were 10.75 MPa and 10.97 MPa, respectively. Until the confining pressure declined to 10.17 MPa, there was no obvious difference between the tangential modulus of the two samples. Thereafter, during the whole unloading process, the tangential modulus of B-2 was consistently greater than that of B-1. For instance, when the confining pressures were 10.5 MPa, 8.5 MPa, and 6.5 MPa, the tangential moduli of B-2 and B-1 were 3.20 GPa, 1.72 GPa, and 0.51 GPa and 2.99 GPa, 1.31 GPa, and 0.35 GPa, respectively.

For convenience, the evolution process of the tangential modulus in this section is only the first cycle of each unloading stage (Figure 9b). Similar to the continuous unloading path, the tangential modulus under the cyclic unloading path is also proportional to the unloading rate. For the first cycle of each unloading stage, when the confining pressures were 8.5 MPa and 5.5 MPa, the tangential moduli of C-2 and C-1 were 2.31 GPa, 0.68 GPa and 2.15 GPa, 0.47 GPa, respectively. However, the tangential modulus changed dramatically between different stages. For example, the tangential modulus of C-1 at the end of the first and second stages was 2.78 GPa and 1.70 GPa, respectively, while at the initial points of the second and third stages, these values were 4.86 GPa and 3.37 GPa, respectively.

To sum up, there is no significant correlation between tangential modulus and unloading rate when confining pressure is in the range of 10–12 MPa, whether it is continuous unloading or cyclic unloading. Once the confining pressure drops below 10 MPa, the tangential modulus under any path is proportional to the unloading rate, that is, the higher the unloading rate, the greater the tangential modulus.

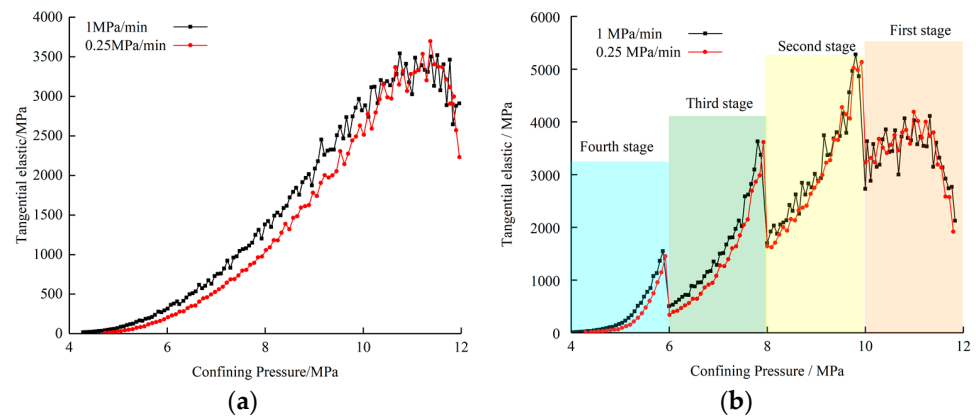


Figure 9. Tangential modulus of tectonic coal: (a) Continuous unloading path; (b) Cyclic unloading path (First cycle of each unloading levels).

4.2. Influence of Unloading Pattern on Deformation and Mechanical Characteristics

4.2.1. Influence on the Strain

Figure 10 and Table 4 show the strains under different paths. As shown in Figure 10a,b, there were no significant differences in the circumferential strain under different unloading modes within the confining pressure range of 12 MPa to 6 MPa. In particular, when the confining pressure dropped from 12 MPa to 7 MPa, the two curves almost completely coincided. When the confining pressure was lower than 7 MPa, the gap between the two curves gradually increased. For example, when the confining pressure was reduced from 6 MPa to 4.5 MPa, the gap between the circumferential strain of B-2 and C-2 increased rapidly from 0.118% to 0.971%.

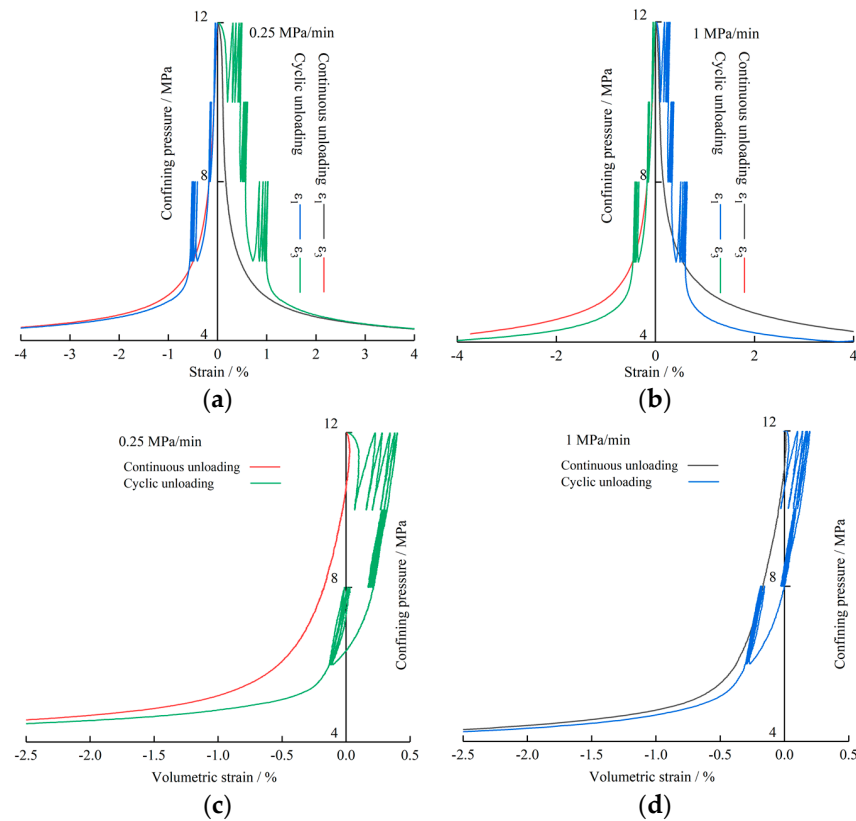


Figure 10. Stress–strain curves under different unloading path: (a) axial and radial strains of B-1 and C-1; (b) axial and radial strains of C-2 and C-2; (c) volume strain of B-1 and C-1; (d) volume strain of B-1 and C-2.

Table 4. Strains under different paths.

Unloading Rate	Confining Pressure/ MPa	Axial Strain/%			Circumferential Strain/%			Volumetric Strain/%		
		UL	CUL		UL	CUL		UL	CUL	
			First Cycle	Fifth Cycle		First Cycle	Fifth Cycle		First Cycle	Fifth Cycle
0.25 MPa/min	10	0.11	0.204	0.443	−0.068	−0.068	−0.072	−0.03	0.068	0.298
	8	0.168	0.467	0.56	−0.17	−0.148	−0.176	−0.171	0.17	0.208
	6	0.462	0.718	0.971	−0.494	−0.409	−0.551	−0.528	−0.1	−0.131
	5.5	0.673	1.032		−0.717		−0.631	−0.76		−0.229
	5	1.113	1.311		−1.184		−0.981	−1.225		−0.649
	4.5	2.41	2.552		−2.659		−2.453	−2.934		−2.355
1 MPa/min	10	0.083	0.099	0.245	−0.064	−0.064	−0.071	−0.044	−0.028	0.102
	8	0.157	0.258	0.324	−0.161	−0.141	−0.165	−0.167	−0.023	−0.007
	6	0.545	0.416	0.591	−0.46	−0.342	−0.443	−0.375	−0.268	−0.297
	5.5	0.839	0.619		−0.666		−0.5	−0.493		−0.381
	5	1.407	0.726		−1.089		−0.665	−0.77		−0.604
	4.5	2.796	1.198		−2.254		−1.283	−1.662		−1.369

Note: UL: Continuous unloading; CUL: Cyclic unloading.

Compared with the circumferential strain, the unloading pattern had a greater impact on the axial strain. Before the confining pressure dropped to 6 MPa, the axial strain increment of the cyclic unloading path was much higher than that of the continuous unloading path. For example, at the end of the first, second, and third unloading stages, the gaps between C-1 and B-1 were 0.333%, 0.392%, and 0.509%, respectively. However, once the unloading entered the fourth stage, the gap decreased quickly. For instance, when the confining pressure was 4.5 MPa, the axial strain difference between C-1 and B-1 was only 0.142%. Moreover, the axial strain of B-2 even exceeded that of C-2 when the confining pressure was lower than 6 MPa. The above results indicate that when the unloading degree is less than 50%, the cycle of unloading is favorable to the increase in axial strain. When the unloading degree is higher than 50%, the axial strain increases faster under the continuous unloading path. Considering that the original sample contained a large number of initial voids, cyclic unloading–loading under high confining pressure conditions was found to be beneficial to the full compression of the sample, thus promoting the growth of axial strain. However, within the continuous decrease in confining pressure, the deviatoric stress exceeded the bearing capacity of the sample and led to the failure of the samples. At this time, the increase in axial strain was caused by the severe damage of the specimen. In other words, the continuous unloading of confining pressure was more conducive to the damage of the sample.

The influence of the unloading pattern on the volumetric strain was mainly manifested in the following aspects. In the initial stage of unloading (confining pressure is higher than 8 MPa), the increase in radial strain is almost not affected by the unloading mode, and the increment of axial strain under the cyclic unloading mode is larger than that of continuous unloading path and the difference is mainly due to the first unloading level of the cyclic unloading path. Therefore, the cyclic unloading mode is more conducive to the volume compression of the sample at this stage. Once the confining pressure is lower than 8 MPa, the axial strain and radial strain increase faster under continuous mode. It is worth noting that, however, the volume strain increases faster in the cyclic unloading mode.

4.2.2. Influence on Tangential Modulus

The evolution of the tangential modulus under different unloading paths was compared in this section to explore the influence of the unloading model on the mechanical properties of tectonic coal, as shown in Figure 11. The tangential modulus of tectonic coal under the cyclic unloading path was higher than when under the continuous unloading path, and the tangential modulus increased significantly with the increase in cycle time during the same unloading stage. For example, when the confining pressures were 9 MPa and 7 MPa, the tangential moduli of B-1 were 2.09 GPa and 0.76 GPa, respectively. For the first and fifth cycles of C-1, these values are 2.88 GPa, 1.49 GPa and 7.09 GPa, 5.31 GPa, respec-

tively. In addition, the evolution of the tangential modulus showed significant differences under different unloading paths. As shown in Table 5, within the cyclic unloading path, the tangential modulus decreased exponentially with the decrease in confining pressure in each unloading stage, whether the first cycle or the fifth cycle. However, the tangential modulus decreased linearly with confining pressure under continuous unloading conditions. Furthermore, compared with continuous unloading, the tangential modulus decreased faster under cyclic unloading.

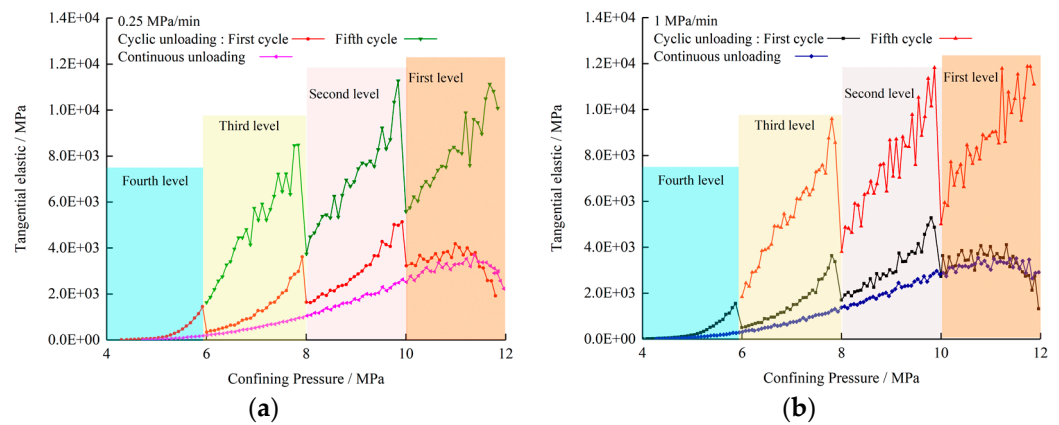


Figure 11. Tangential modulus of tectonic coal under different unloading path: (a) B-1 and C-1; (b) B-2 and C-2.

Table 5. Fitting relationship between tangent modulus and confining pressure.

Confining Pressure/ MPa	Fitting Function					
	Cyclic Unloading				Continuous Unloading	
	First Cyclic	R ²	Fifth Cyclic	R ²		R ²
12–10	/		$E_T = 207.45 \exp(0.34\sigma_3)$	0.97	/	
10–8	$E_T = 11.49 \exp(0.61\sigma_3)$	0.98	$E_T = 110.80 \exp(0.46\sigma_3)$	0.97	$E_T = (0.81\sigma_3 - 5.51) \times 10^3$	0.98
8–6	$E_T = 0.30 \exp(1.18\sigma_3)$	0.99	$E_T = 25.49 \exp(0.75\sigma_3)$	0.94	$E_T = (0.41\sigma_3 - 2.31) \times 10^3$	0.99
6–4	$E_T = 2 \times 10^{-5} \exp(3.10\sigma_3)$	0.99	/		$E_T = (0.14\sigma_3 - 0.69) \times 10^3$	0.98

The above results indicate that the tangent modulus of samples under the cyclic unloading model is much higher than that under the continuous unloading path. Moreover, at the same unloading level, the tangential modulus increases by 200–300% with an increase in the number of cycles, and the higher the unloading rate, the larger the increase in tangential modulus. This is because during the process of repeated loading–unloading of confining pressure, the void between coal particles is constantly compressed, and the meshing between the particles becomes closer. As a result, the ability of resistance to deformation is enhanced at the macro level.

In addition, the decline rate of tangent modulus in the cyclic unloading mode is also much higher than that in the continuous unloading path. The mechanism of this phenomenon will be discussed later.

4.3. Poisson Ratio under Cyclic Unloading Path

The Poisson ratio is the ratio of circumferential strain to axial strain, which reflects the progressive damage to the materials during plastic deformation processes. Based on the test results, the Poisson ratio was observed to change with the number of cycles under different rates of cyclic unloading paths. In this study, the calculation method referred to that of Peng et al. [26]; the Poisson ratios of the tectonic coal are plotted in Figure 12, and they generally exhibited a stepwise rising trend.

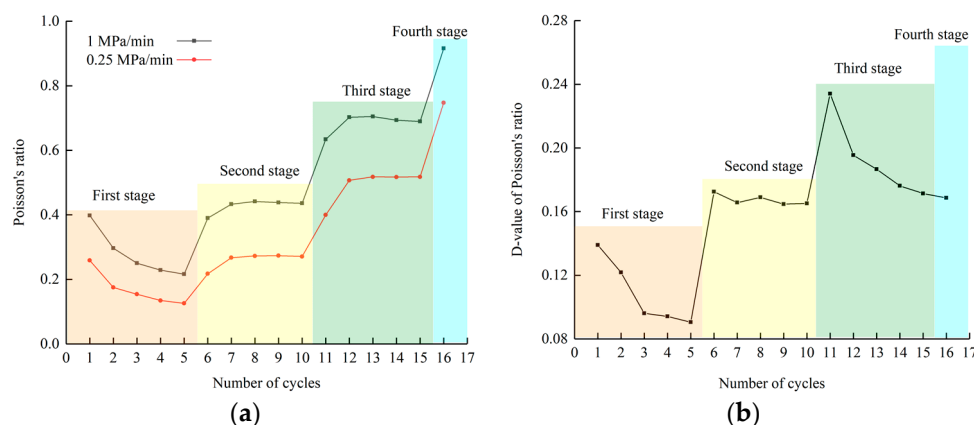


Figure 12. (a) Poisson's ratio under cyclic unloading path; (b) The gap of Poisson's ratio between C-1 and C-2.

In the first stage of the cyclic unloading process, the Poisson ratio continued to decrease with the increase in the number of cycles. This is because the tectonic coal was compacted in the axial direction during the initial stage, while the high confining pressure limited the circumferential strain of the specimen. In the second unloading stage, the continuous unloading of the confining pressure resulted in micro-fractures occurring in this process. At this moment, the growth of the circumferential strain began to accelerate, and the Poisson ratio gradually increased from 0.126 and 0.217 to 0.218 and 0.391, respectively. With the further unloading of the confining pressure, micro-crack development caused a plastic deformation from the macro perspective. Furthermore, in the third unloading stage of the cyclic unloading path, the Poisson ratio increased sharply, owing to the failure of the specimen; the Poisson ratio of C-1 and C-2 increased to 0.633 and 0.399, respectively. The Poisson ratio remained near a relatively stable value during the last four cycles in each stress level, and the tectonic coal seemed to enter the elastic phase in this process.

In addition, different unloading rates resulted in varying effects. The increase in the unloading rate provided the tectonic coal with stronger hardening properties and inhibited the increase in the axial deformation, resulting in less axial deformation in C-1. This explains why the Poisson ratio of C-1 was higher than that of C-2. With the increase in the deviatoric stress level, the Poisson ratio gap between the different stages was significantly increased; this phenomenon can be clearly observed in Figure 12b. However, during the last four cycles of each unloading stage, the gap between the Poisson ratio of C-1 and C-2 tended to decrease. This is because the lower unloading rate was conducive to the growth of both axial and circumferential strain. When the confining pressure was repeatedly unloaded–loaded within a fixed range, the circumferential strain had a higher growth ratio than the axial strain.

4.4. Investigation of the Mechanisms

The samples used in this study were moulded using coal particles of different sizes under high pressure. Figure 13 shows the CT scan results of an intact sample and a failure sample. In contrast to the brittle failure of the intact coal, there was no obvious continuous crack in the failure of the tectonic coal; the sliding between the grains is the nature of tectonic damage.

In this experiment, the confining pressure was unloaded while the axial pressure remained unchanged. There were two effects in the unloading process: a reduction in confining pressure and an increase in deviatoric stress, both of which are beneficial to material damage. Therefore, the axial and circumferential strains increased significantly with the decrease in confining pressure. Moreover, Peng et al. suggested that rapid changes in stress lead to a shortened disturbance time for the external force, so the moving distance of grains will be greatly decreased [27]. On the contrary, if the change rate is low, the dislocation of the internal coal grains in the sample will be more plentiful [28]. Therefore, as

shown in Figure 13, whether continuous (Figure 14a–c) or cyclic unloading (Figure 14d–f), the lower the unloading rate, the higher the strain rate.

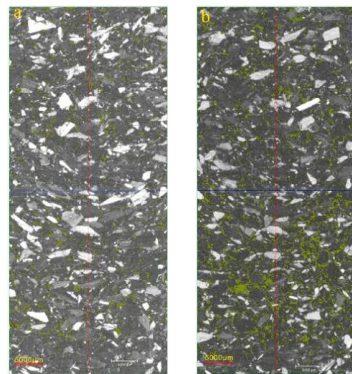


Figure 13. CT scan results. (a) Initial sample; (b) Failure sample.

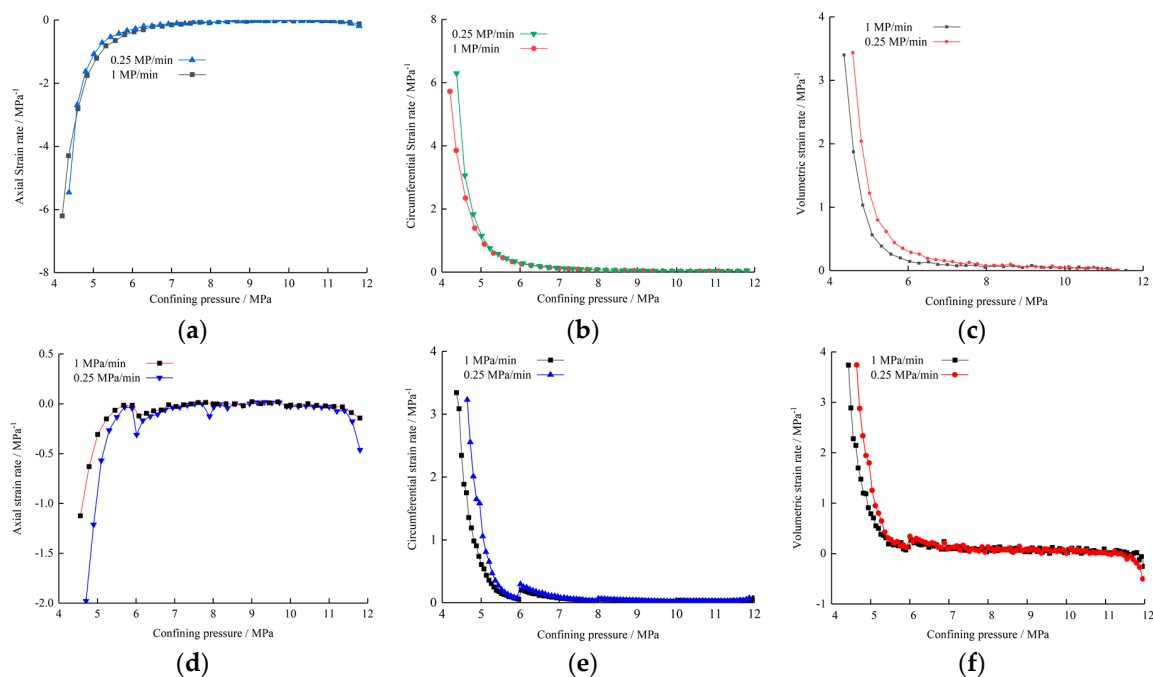


Figure 14. Strain rate of tectonic coal under different unloading rate. Continuous unloading path—(a) axial strain rate, (b) circumferential strain rate, (c) volume strain rate; Cyclic unloading path—(d) axial strain rate, (e) circumferential strain rate, (f) volume strain rate.

This theory can also explain why the lower unloading rate under the cyclic unloading path was conducive to both compression under a high confining pressure and expansion under a low confining pressure. During the initial stage of unloading, a large number of initial voids were compressed sufficiently due to the prolonged disturbance time of the deviatoric force. In the dilatation process, low-speed unloading lengthened the lateral displacement distance of particles, resulting in a larger volume expansion.

Under the cyclic path, the deviatoric stress circulated repeatedly within the same range during each unloading stage. According to the Kaiser effect, the original crack will close under the stress drive (instead of causing further damage) if the subsequent load does not reach the previous stress level [29]. As observed in the stress–strain curve of the cyclic unloading experiment, there was no obvious plastic deformation prior to the confining pressure being lower than 6 MPa. Therefore, in the cyclic unloading–loading process, the adaptive adjustment of the coal particles leads to the continuous compression of the interspace between particles [28], which results in the slow growth of the axial and

circumferential strains. Furthermore, with the increase in the compression degree, the amount of compression caused by a single cycle gradually decreases.

Due to defects inside the tectonic coal specimens becoming gradually closed, the internal structure became denser. This seems to be a “self-healing” process of the specimen and macroscopically implies that the tangential modulus increased remarkably. Once the first cycle of the next unloading stage began, however, the deviatoric stress exceeded the previous stress level. At this time, new damage began to appear, and the original damage expanded or became connected, which led to a rapid increase in the three types of strain.

It is worth noting that, except for the first unloading stage (the first cycle in the first unloading stage was equivalent to continuous unloading), although the strain rate for the first cycle of each unloading stage was lower than that in the continuous unloading path, the growth of the strain rate was higher than that of continuous unloading (Figure 15). From an energy accumulation and release perspective, the elastic energy was accumulated in the sample due to volume compression during the cyclic process. With the further unloading of the confining pressure, these energies will be released and promote the damage of the sample [30]. Therefore, the increase in deviatoric stress was accompanied by the release of energy in this process, which resulted in a faster increase in the strain rate. Moreover, Zhao et al. suggested that, during the stress cycle, this may result in loosened grains [31], which also promotes the increase in strain rate and the decrease in tangential modulus. Therefore, the decreasing rate of the tangential modulus under the cyclic unloading path was higher than that under the continuous unloading path.

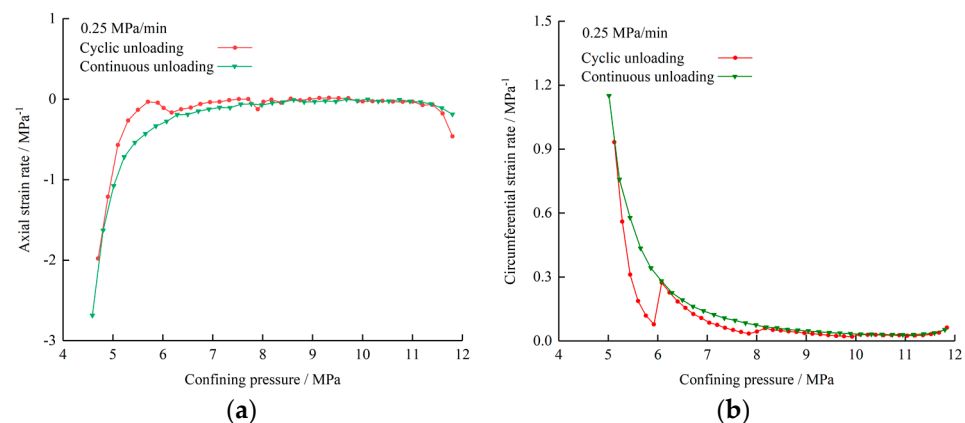


Figure 15. Growth of strain rate under different unloading pattern: (a) axial strain rate; (b) circumferential strain rate.

4.5. Reference Meaning for Engineering

The continuous unloading pattern results in the incessant expansion of the volume during the whole unloading process, and a lower unloading rate is conducive to the volume expansion. This unloading pattern has strong timeliness and a positive significance for improvements to the permeability of reservoirs, which is conducive to the extraction of coalbed methane. However, the rapid volume expansion of tectonic coal can induce the violent destruction of the borehole, which is unfavorable to the stable and sustainable extraction of coalbed methane. For cyclic unloading, a lower unloading rate is beneficial to the compression of tectonic coal in the initial unloading stage. Previous experimental results have shown that the permeability of the sample is reduced with an increase in the number of loading and unloading cycles under relatively high confining pressures [19,32–35], which is extremely unfavorable for the extraction of coalbed methane. However, the research results of this study showed that the cyclic unloading path is beneficial to delaying the damage (even “repairing” the damage to a certain extent) and improving the mechanical strength of the tectonic coal. This makes it easier to maintain the stability of the borehole when the confining pressure is greatly reduced.

Therefore, in engineering applications, the two unloading patterns can be combined to effectively and controllably induce pressure relief in the tectonic coal reservoir. Initially, low-rate continuous unloading was adopted to improve the permeability of the reservoir, and then high-speed cyclic unloading was adopted to suppress the damage to the tectonic coal so as to avoid severe hole collapses and to guarantee the sustainability of gas extraction.

5. Conclusions

1. Whether using cyclic unloading or continuous unloading, the compression effect was found to be dominant when the unloading level was small. When the unloading level was large, continuous unloading was more conducive to the volume expansion of tectonic coal than cyclic unloading. The strain was inversely proportional to the unloading rate, and the tangential modulus was directly proportional to the unloading rate, whether using continuous unloading or cyclic unloading.

2. Irreversible strain of cyclic unloading in most of the unloading levels mainly occurred in the first cycle, but to a lesser extent in subsequent cycles. The strain memory during the confining pressure of the cyclic loading led to the adaptive adjustment of the particles, and the tangential modulus in the cyclic unloading process was higher than that in the continuous unloading process.

3. During the reciprocation of the unloading–loading of the confining pressure, some elastic energy was accumulated in the sample and was released in the first cycle of the subsequent unloading stage. However, for the continuous unloading of the confining pressure, there was no such energy accumulation process. Therefore, the increase rate of the strain rate and the decrease rate of the tangential modulus of the tectonic coal were higher under the cyclic unloading path.

4. Continuous unloading plays a positive role in improving reservoir permeability, while cyclic unloading was found to inhibit damage expansion and to improve the strength of tectonic coal. A reasonable combination of the two unloading patterns may be beneficial for pressure relief purposes in tectonic coal reservoirs and for the extraction of coalbed methane.

Author Contributions: Conceptualization, S.S.; Data curation, D.G., W.W. and H.M.; Formal analysis, S.L. and W.W.; Investigation, D.G. and H.M.; Methodology, D.G.; Project administration, S.S.; Resources, S.S. and S.L.; Writing—original draft, D.G., S.L., W.W. and H.M.; Writing—review & editing, D.G. All authors have read and agreed to the published version of the manuscript.

Funding: This research was funded by National Major Scientific Research Instrument Development Project (No. 41727801), the National Natural Science Foundation of China Grant (No. 42030810), the Dominant discipline support project of Jiangsu Province (No. 2020CXNL11), the National Natural Science Foundation of China (No. 41972168), and the Foundation of Jiangsu Key Laboratory of Coal-based Greenhouse Gas Control and Utilization (No. 2020ZDZZ01D).

Data Availability Statement: Data is unavailable due to privacy or ethical restrictions.

Conflicts of Interest: The authors declare no conflict of interest.

References

1. Mark, C.; Gauna, M. Evaluating the risk of coal bursts in underground coal mines. *Int. J. Min. Sci. Technol.* **2016**, *26*, 47–52. [[CrossRef](#)]
2. Wang, H.; Xu, W.; Cai, M.; Xiang Kong, Z. Gas permeability and porosity evolution of a porous sandstone under repeated loading and unloading conditions. *Rock Mech. Rock. Eng.* **2017**, *50*, 2071–2083. [[CrossRef](#)]
3. Soofastaei, A.; Aminossadati, S.M.; Kizil, M.S.; Knights, P. A comprehensive investigation of loading variance influence on fuel consumption and gas emissions in mine haulage operation. *Int. J. Min. Sci. Technol.* **2016**, *26*, 995–1001. [[CrossRef](#)]
4. Pan, Z.; Connell, L.D. Modelling of anisotropic coal swelling and its impact on permeability behaviour for primary and enhanced coalbed methane recovery—ScienceDirect. *Int. J. Coal Geol.* **2011**, *85*, 257–267. [[CrossRef](#)]
5. Qin, L.; Wang, P.; Li, S.; Lin, H.; Ma, C. Gas adsorption capacity changes in coals of different ranks after liquid nitrogen freezing. *Fuel* **2021**, *292*, 120404. [[CrossRef](#)]

6. Chao, Z.; Ma, G.; Wang, M. The investigation of seepage model for columnar jointed rock masses during cyclic loading and unloading of confining pressure. *Arab. J. Geosci.* **2020**, *13*, 621. [[CrossRef](#)]
7. Browning, J.; Meredith, P.G.; Stuart, C.E.; Healy, D.; Harland, S.; Mitchell, T.M. Acoustic characterization of crack damage evolution in sandstone deformed under conventional and true triaxial loading. *J. Geophys. Res. Solid Earth* **2017**, *122*, 4395–4412. [[CrossRef](#)]
8. Taheri, A.; Yfantidis, N.; Olivares, C.L.; Connelly, B.J.; Bastian, T.J. Experimental study on degradation of mechanical properties of sandstone under different cyclic loadings. *Geotech. Test. J.* **2016**, *39*, 673–687. [[CrossRef](#)]
9. Adushkin, V.V.; Kocharyan, G.G.; Ostapchuk, A.A. Parameters determining the portion of energy radiated during dynamic unloading of a section of rock massif. *Dokl. Earth Sci.* **2016**, *467*, 275–279. [[CrossRef](#)]
10. Sun, L.; Zhang, L.; Cong, Y.; Song, Y.; He, K. The meso-fracturing mechanism of marble under unloading confining pressure paths and constant axial stress. *Sci. Rep.* **2021**, *11*, 17835. [[CrossRef](#)]
11. Zhang, D.M.; Yang, Y.S.; Chu, Y.P.; Zhang, X.; Xue, Y.G. Influence of loading and unloading velocity of confining pressure on strength and permeability characteristics of crystalline sandstone. *Results Phys.* **2018**, *9*, 1363–1370. [[CrossRef](#)]
12. Ma, T.; Ma, D.; Yang, Y. Fractal Characteristics of Coal and Sandstone Failure under Different Unloading Confining Pressure Tests. *Adv. Mater. Sci. Eng.* **2020**, *2020*, 2185492. [[CrossRef](#)]
13. Xue, Y.; Ranjith, P.G.; Gao, F.; Zhang, D.; Cheng, H.; Chong, Z.; Hou, P. Mechanical behaviour and permeability evolution of gas-containing coal from unloading confining pressure tests. *J. Nat. Gas Sci. Eng.* **2017**, *40*, 336–346. [[CrossRef](#)]
14. Zhang, M.; Lin, M.; Zhu, H.; Zhou, D.; Wang, M. An experimental study of the damage characteristics of gas-containing coal under the conditions of different loading and unloading rates—ScienceDirect. *J. Loss Prev. Process Ind.* **2018**, *55*, 338–346. [[CrossRef](#)]
15. Yin, G.; Jiang, C.; Wang, J.G.; Jiang, X. Geomechanical and flow properties of coal from loading axial stress and unloading confining pressure tests. *Int. J. Min. Sci. Technol.* **2015**, *76*, 155–161. [[CrossRef](#)]
16. Jiang, C.; Yang, Y.; Wei, W.; Duan, M.; Yu, T. A new stress-damage-flow coupling model and the damage characterization of raw coal under loading and unloading conditions. *Int. J. Min. Sci. Technol.* **2021**, *138*, 104601. [[CrossRef](#)]
17. Pan, R.; Fu, D.; Yu, M.; Chen, L. Directivity effect of unloading bedding coal induced fracture evolution and its application. *Int. J. Min. Sci. Technol.* **2017**, *27*, 825–829.
18. Zhao, H.; Wang, J. Experimental study of evolution law of mechanical properties of coal containing gas under unloading confining pressure. *Yantu Lixue/Rock Soil Mech.* **2011**, *32*, 270–274.
19. Yang, Y.; Jiang, C.; Guo, X.; Peng, S.; Zhao, J.; Yan, F. Experimental investigation on the permeability and damage characteristics of raw coal under tiered cyclic unloading and loading confining pressure. *Powder Technol.* **2021**, *389*, 416–429. [[CrossRef](#)]
20. Zhou, H.; Wang, L.; Rong, T.; Zhang, L.; Ren, W.; Su, T. Creep-based permeability evolution in deep coal under unloading confining pressure. *J. Nat. Gas Sci. Eng.* **2019**, *65*, 185–196. [[CrossRef](#)]
21. Chen, W.; Lv, S.; Guo, X.; Qiao, C. Research on unloading confining pressure tests and rock burst criterion based on energy theory. *Chin. J. Rock Mech. Eng.* **2009**, *28*, 1530–1540.
22. Sang, S.; Zhou, X.; Liu, S.; Wang, H.; Cao, L.; Liu, H.; Li, Z.; Zhu, S.; Liu, C.; Huang, H.; et al. Research advances in theory and technology of the stress release applied extraction of coalbed methane from tectonically deformed coals. *J. China Coal Soc.* **2020**, *45*, 2531–2543.
23. Lu, S.; Cheng, Y.; Li, W.; Wang, L. Pore structure and its impact on CH₄ adsorption capability and diffusion characteristics of normal and deformed coals from Qinshui Basin. *Int. J. Oil Gas Coal Technol.* **2015**, *10*, 76–78. [[CrossRef](#)]
24. Geng, J.; Cao, L.; Zhong, C.; Zhang, S. An Experimental Study on Preparation of Reconstituted Tectonic Coal Samples: Optimization of Preparation Conditions. *Energies* **2021**, *14*, 2846. [[CrossRef](#)]
25. Taheri, A.; Tatsuoka, F. Small- and large-strain behaviour of a cement-treated soil during various loading histories and testing conditions. *Acta Geotech* **2015**, *10*, 131–155. [[CrossRef](#)]
26. Peng, K.; Zhou, J.; Zou, Q.; Zhang, J.; Wu, F. Effects of stress lower limit during cyclic loading and unloading on deformation characteristics of sandstones. *Constr. Build. Mater.* **2019**, *217*, 202–215. [[CrossRef](#)]
27. Peng, K.; Zhou, J.; Zou, Q.; Song, X. Effect of loading frequency on the deformation behaviours of sandstones subjected to cyclic loads and its underlying mechanism. *Int. J. Fatigue* **2020**, *131*, 105349. [[CrossRef](#)]
28. Wang, J.; Zhang, Q.; Song, Z.; Zhang, Y. Experimental study on creep properties of salt rock under long-period cyclic loading. *Int. J. Fatigue* **2021**, *143*, 106009. [[CrossRef](#)]
29. Yin, X.; Li, S. Study on measurement of in-situ stress with Kaiser effect of rock acoustic emission. *Min. Technol.* **2006**, *6*, 278–280.
30. Munoz, H.; Taheri, A.; Chanda, E.K. Rock Drilling Performance Evaluation by an Energy Dissipation Based Rock Brittleness Index. *Rock Mech. Rock Eng.* **2016**, *49*, 3343–3355. [[CrossRef](#)]
31. Zhao, Y.; Bi, J.; Wang, C.; Liu, P. Effect of Unloading Rate on the Mechanical Behavior and Fracture Characteristics of Sandstones Under Complex Triaxial Stress Conditions. *Rock Mech. Rock Eng.* **2021**, *54*, 4851–4866. [[CrossRef](#)]
32. Kan, Z.; Zhang, L.; Li, M.; Yuan, X.; Huang, M. Investigation of Seepage Law in Broken Coal and Rock Mass under Different Loading and Unloading Cycles. *Geofluids* **2021**, *2021*, 8127250. [[CrossRef](#)]
33. Xin, T.; Liang, B.; Wang, J.; Sun, W.; Sun, Y. Experimental Study on the Evolution Trend of the Pore Structure and the Permeability of Coal under Cyclic Loading and Unloading. *ACS Omega* **2021**, *6*, 35830–35843. [[CrossRef](#)] [[PubMed](#)]

34. Wang, K.; Guo, Y.; Xu, H.; Dong, H.; Du, F.; Huang, Q. Deformation and permeability evolution of coal during axial stress cyclic loading and unloading: An experimental study. *Geomech. Eng.* **2021**, *24*, 519–529.
35. Zhang, C.; Zhang, L. Permeability Characteristics of Broken Coal and Rock Under Cyclic Loading and Unloading. *Nat. Resour. Res.* **2019**, *28*, 1055–1069. [[CrossRef](#)]

Disclaimer/Publisher’s Note: The statements, opinions and data contained in all publications are solely those of the individual author(s) and contributor(s) and not of MDPI and/or the editor(s). MDPI and/or the editor(s) disclaim responsibility for any injury to people or property resulting from any ideas, methods, instructions or products referred to in the content.